Interface effects on the dielectric response of a multiple-quantum-wire lattice and current-driven plasmon instability

2004 J. Phys.: Condens. Matter 16 2215

(http://iopscience.iop.org/0953-8984/16/13/003)

INSTITUTE OF PHYSICS PUBLISHING JOURNAL OF PHYSICS: CONDENSED MATTER

J. Phys.: Condens. Matter **16** (2004) 2215–2230 PII: S0953-8984(04)71889-5

Interface effects on the dielectric response of a multiple-quantum-wire lattice and current-driven plasmon instability

Norman J M Horing[1], **Vassilios Fessatidis**[2] **and Yuksel Ayaz**[1]

[1] Department of Physics and Engineering Physics, Stevens Institute of Technology, Hoboken, NJ 07030, USA
[2] Physics Department, Fordham University, Bronx, NY 10458, USA

E-mail: fessatidis@fordham.edu

Received 12 November 2003
Published 19 March 2004
Online at stacks.iop.org/JPhysCM/16/2215 (DOI: 10.1088/0953-8984/16/13/003)

Abstract

We have determined the nonlocal, dynamic dielectric response properties of a multiple-quantum-wire lattice embedded in a semi-infinite plasma-like host medium, with the progression of parallel wires perpendicular to the interface, while the wires themselves are parallel to the surface. This is carried out within the framework of the random phase approximation, neglecting tunnelling. In this study, we have also investigated the condition for the occurrence of current-driven plasmon instability as a function of z_0, the distance of the first quantum wire from the bounding surface, and as a function of a, the separation of the quantum wires. Furthermore, the coupled mode dispersion relations for the plasmons of multiple-quantum-wire systems in interaction with the surface and bulk plasmons of the host material are analysed for dependences on the geometrical parameters z_0 and a.

1. Introduction

Developments in nanostructure science and technology over the past decade have focused much attention on the dielectric response properties [1–3] of very small nanosystems. In particular, quantum-wire plasmons have been investigated [4–12] with multiple wires embedded in a bulk semiconductor, and single-wire systems have been examined in the vicinity of an interface [13–15]. Here, we report on our analysis of the inverse dielectric function and plasmon spectrum of multiple-quantum-wire lattices embedded in a semi-infinite plasma-like host semiconductor having a mobile electron population that may be due to excessive doping or real-space transfer. The wires are parallel to each other and to the bounding surface, while the progression of wires is perpendicular to the surface (figure 1). The electrostatic collective modes examined are constituted of the hybridization of the quantum-wire plasmons coupled

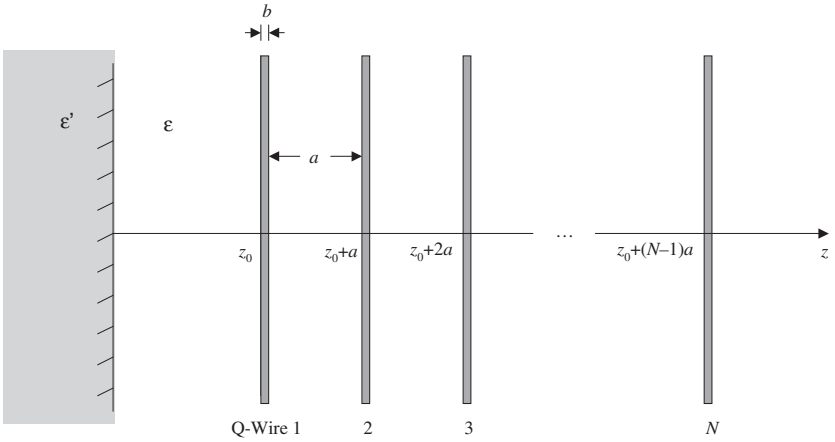

Figure 1. A system of N quantum wires with spacing a and width b, with the first at a distance z_0 from the interface at $z = 0$ of the semi-infinite host medium of dielectric constant $\varepsilon(\omega)$ with a medium of dielectric constant ε' on the other side.

to the bulk and surface plasmons of the host medium, with internal Coulomb coupling among the wire plasmons. The dispersion of the modes is determined as a function of wavenumber parallel to the wires (which are equally spaced by distance a) and as a function of the distance of the first wire from the interface, z_0 (figure 1).

Recently reported experiments [16, 17] and theoretical considerations [18] have underscored the importance of multiple (double) planar quantum well nano-systems in the detection of terahertz radiation by means of resonant plasmon and current response with a grating coupler. Furthermore, it has now been shown [19] that current driven plasmon instability can also occur in a double-quantum-wire system carrying equal and opposite currents in the two wires, provided that the drift velocity falls between the acoustic and optical phase velocities of the double-quantum-wire plasmons. In consideration of these accomplishments, and with an eye toward mechanisms for optimization of such features for possible use in terahertz devices, we also explore here the effects of the interface under consideration on the criterion for double-quantum-wire plasmon instability—in particular as it relates to dependences on z_0 (distance of the first wire from the interface) and a (separation of the wires).

2. Polarizabilities of a semi-infinite plasma-like host medium ($\alpha^0_{\mathbf{semi}}$) and of N quantum wires ($\alpha^0_{\mathbf{NQW}}$)

Within the framework of the random phase approximation (RPA—neglecting tunnelling), the polarizability of the combined system of a semi-infinite host medium and N quantum wires embedded in it is quite accurately given by the sum of the polarizabilities of the constituent parts [20], $\alpha = \alpha^0_{\rm semi} + \alpha^0_{\rm NQW}$, where $\alpha^0_{\rm semi}$ represents the polarizability of the bounded plasma-like host medium (continuum band) and $\alpha^0_{\rm NQW}$ refers to the polarizability of the N-quantum-wire system. The local polarizability for the semi-infinite plasma-like dielectric medium (continuum band) is given in position z-representation as [14] (here we allow that the adjoining medium has a dielectric constant ε' different from $\varepsilon = \varepsilon_0 - \omega_{\rm p}^2/\omega^2$ with which we model the host dielectric properties, with ε_0 as the background dielectric constant and $\omega_{\rm p} = (4\pi e^2 n_{\rm 3D}/m)^{1/2}$

as the classical bulk plasma frequency of the semi-infinite host plasma continuum band)

$$\alpha^0_{\rm semi}(\bar{\mathbf{q}},\omega;z_3,z_2)=\delta(z_3-z_2)[\eta_+(z_3)-1]+(\varepsilon'-\varepsilon)\delta(z_2)\eta_-(z_3)\mathrm{e}^{-\bar{q}|z_3|}/2, \tag{1}$$

where $\bar{\mathbf{q}}\equiv(q_x,q_y)$ is the two-dimensional wavevector in the lateral plane. Here, we have defined $\eta_-(z)=\theta(z)-\theta(-z)=1,0,-1$ for $z>0,z=0,z<0$, and $\eta_+(z)=\varepsilon\theta(z)+\varepsilon'\theta(-z)=\varepsilon,(\varepsilon'+\varepsilon)/2,\varepsilon'$ for $z>0,z=0,z<0$, respectively. ($\theta(z)$ denotes the Heaviside unit step function, $\theta(z)=1$ for $z>0$, $1/2$ for $z=0$, and 0 for $z<0$.) Notwithstanding its spatial translational invariance in the y-direction it is necessary to transform $\alpha^0_{\rm semi}(\bar{\mathbf{q}},\omega;z_3,z_2)$ to a y-representation to accommodate the description of quantum wires confined in the y-direction of the lateral plane. Therefore, we Fourier transform back into y-position representation, writing

$$\begin{aligned}\alpha^0_{\rm semi}(q_x,\omega;y_3z_3,y_2z_2)&=\int\frac{\mathrm{d}q_y}{2\pi}\mathrm{e}^{\mathrm{i}q_y(y_3-y_2)}\alpha^0_{\rm semi}(q_x,q_y,\omega;z_3,z_2)\\&=\delta(y_3-y_2)\delta(z_3-z_2)[\eta_+(z_3)-1]+\delta(z_2)\eta_-(z_3)|z_3|(\varepsilon'-\varepsilon)\\&\quad\times\left(\frac{|q_x|}{2\pi}\right)\left(\frac{\mathrm{K}_1\left(|q_x|\sqrt{(y_2-y_3)^2+z_3^2}\right)}{\sqrt{(y_2-y_3)^2+z_3^2}}\right),\end{aligned} \tag{2}$$

where $|q_x|$ is the magnitude of the one-dimensional (1D) wavevector conjugate to the translationally invariant x-axis and $\mathrm{K}_1(z)$ is the modified Bessel function of order one.

Assuming that there is no tunnelling, the joint polarizability of the N quantum wires is given by the sum of polarizabilities of the individual wires [20]:

$$\alpha^0_{\rm NQW}=\sum_{\sigma=0}^{N-1}\alpha^\sigma(3,2), \tag{3}$$

where

$$\alpha^\sigma(3,2)=-\int\mathrm{d}1\,v(3,1)R^\sigma(1,2) \tag{4}$$

is the free electron polarizability of the σth quantum wire. Here, $v(3,1)$ is the Coulomb potential and $R^\sigma(1,2)=-\mathrm{i}G^\sigma(1,2)G^\sigma(2,1)$ is the ring diagram density perturbation response function. Here, $G^\sigma(1,2)$ denotes the noninteracting (one-electron) thermodynamic Green function for the σth wire. Fourier transforming along the translationally invariant x-axis parallel to the quantum wires, $x_1-x_2\to q_x$, and in time, $t_1-t_2\to\omega$, we have

$$\alpha^\sigma(y_3z_3,y_2z_2;q_x,\omega)=-\int\mathrm{d}y_1\int\mathrm{d}z_1\,v(y_3-y_1,z_3-z_1;q_x,\omega)R^\sigma(y_1z_1,y_2z_2;q_x,\omega), \tag{5}$$

where $v(y_3-y_1,z_3-z_1;q_x,\omega)$ is the Fourier transform of the 1D Coulomb potential,

$$v(y_3-y_1,z_3-z_1;q_x,\omega)=2e^2\mathrm{K}_0\left(|q_x|\sqrt{(y_3-y_1)^2+(z_3-z_1)^2}\right), \tag{6}$$

$|q_x|$ is the magnitude of the 1D wavevector and $\mathrm{K}_0(z)$ represents the modified Bessel function of order zero.

The noninteracting thermodynamic Green function for each of the disjoint wires having only the lowest sub-band in the y-direction energetically accessible, and n sub-bands in the z-direction, can be written in terms of orthonormal sub-band wavefunctions as

$$\begin{aligned}\mathrm{i}G^\sigma(\mathbf{r_1},\mathbf{r_2};t_1,t_2)&=\sum_{\alpha=1}^{n}\int\frac{\mathrm{d}q_x}{2\pi}\,\mathrm{e}^{\mathrm{i}q_x(x_1-x_2)}\mathrm{e}^{-\mathrm{i}(\epsilon_{q_x}+E_{\alpha\sigma})(t_1-t_2)}\phi^\sigma_\alpha(y_1,z_{1\sigma})\phi^\sigma_\alpha(y_2,z_{2\sigma})\\&\quad\times\begin{cases}1-f_0(\epsilon_{q_x}+E_{\alpha\sigma}) & \text{for } t_1>t_2\\ -f_0(\epsilon_{q_x}+E_{\alpha\sigma}) & \text{for } t_1<t_2,\end{cases}\end{aligned} \tag{7}$$

where $\phi^{\sigma}_{\alpha} = \chi(y_1)\xi^{\sigma}_{\alpha}(z_{1\sigma})$ denotes a (real) quantized sub-band wavefunction due to confinement of electrons in the y- and z-directions, in the σth wire, with a coordinate $z_{1\sigma}$ relative to the wire centre, $z_{1\sigma} = z_1 - z_{0\sigma}$ ($z_{0\sigma} = z_0 + \sigma a$; $\sigma = 0, 1, 2, \ldots, N-1$), and $E_{\alpha\sigma} = E_{\alpha\sigma(z)} + E_{(y)}$ denotes the corresponding quantized sub-band energy. ($E_{\alpha\sigma(z)}$ represents the sub-band energy in the z-direction and $E_{(y)}$ is the lowest sub-band energy in the y-direction.) We note that the lowest sub-band wavefunction $\chi(y_1)$ does not depend on the wire index σ—as assumed above—but we retain the capacity to describe an asymmetric quantum wire system by having the z-sub-band wavefunction depend on σ. $f_0(\epsilon_{q_x} + E_{\alpha\sigma})$ is the mean occupation number (Fermi distribution) of electrons in the α sub-band of the σth wire, $f_0(\epsilon_{q_x} + E_{\alpha\sigma}) = [1 + \exp((\epsilon_{q_x} + E_{\alpha\sigma} - E_{\mathrm{F}\sigma})/k_{\mathrm{B}}T)]^{-1}$ with chemical potential $E_{\mathrm{F}\sigma}$ (k_{B} is the Boltzmann constant and T is the absolute temperature) and $\epsilon_{q_x} = \hbar^2 q_x^2/2m$ refers to the part of the single-electron kinetic energy along the x-axis of the σth quantum wire. Fourier transforming along the translationally invariant x-axis, we determine $R^{\sigma}(y_1 z_1, y_2 z_2; q_x, \omega)$ in the form

$$R^{\sigma}(y_1 z_1, y_2 z_2; q_x, \omega) = \sum_{\alpha,\beta} R^{\sigma}_{\alpha\beta}(q_x, \omega)\Phi^{\sigma}_{\alpha\beta}(y_1, z_1; y_2, z_2), \tag{8}$$

where the matrix element of the 'ring diagram' density perturbation response function $R^{\sigma}_{\alpha\beta}(q_x, \omega)$ of the σth wire with sub-band indices α, β is given by

$$R^{\sigma}_{\alpha\beta}(q_x, \omega) = 2\int \frac{\mathrm{d}q'_x}{2\pi} \frac{f_0(\epsilon_{q'_x - q_x} + E_{\beta\sigma}) - f_0(\epsilon_{q'_x} + E_{\alpha\sigma})}{\omega + \epsilon_{q'_x - q_x} - \epsilon_{q'_x} + (E_{\beta\sigma} - E_{\alpha\sigma}) + \mathrm{i}0^+}, \tag{9}$$

and $\Phi^{\sigma}_{\alpha\beta}(y_1, z_1; y_2, z_2)$ is given by

$$\Phi^{\sigma}_{\alpha\beta}(y_1, z_1; y_2, z_2) = \phi^{\sigma}_{\alpha}(y_1, z_{1\sigma})\phi^{\sigma}_{\alpha}(y_2, z_{2\sigma})\phi^{\sigma}_{\beta}(y_1, z_{1\sigma})\phi^{\sigma}_{\beta}(y_2, z_{2\sigma}). \tag{10}$$

Summing the constituent polarizabilities, $\alpha^0_{\mathrm{semi}} + \alpha^0_{\mathrm{NQW}}$, we obtain the joint polarizability, α, of the combined N-quantum-wire system with the semi-infinite host plasma (in y-representation) as

$$\begin{aligned}\alpha(y_3 z_3, y_2 z_2; q_x, \omega) &= \delta(y_3 - y_2)\delta(z_3 - z_2)[\eta_+(z_3) - 1] \\ &+ \delta(z_2)\eta_-(z_3)|z_3|(\varepsilon' - \varepsilon)\left(\frac{|q_x|}{2\pi}\right)\left(\frac{\mathrm{K}_1\left(|q_x|\sqrt{(y_2 - y_3)^2 + z_3^2}\right)}{\sqrt{(y_2 - y_3)^2 + z_3^2}}\right) \\ &- 2e^2 \sum_{\alpha,\beta}\sum_{\sigma} R^{\sigma}_{\alpha\beta}(q_x, \omega)V^{\sigma}_{\alpha\beta}(y_3, z_3)\phi^{\sigma}_{\alpha}(y_2, z_{2\sigma})\phi^{\sigma}_{\beta}(y_2, z_{2\sigma}),\end{aligned} \tag{11}$$

where we define the matrix element of the Fourier transform of the 1D Coulomb potential (modified Bessel function of order zero) with sub-band indices α, β and wire index σ by

$$V^{\sigma}_{\alpha\beta}(y_3, z_3) = \int \mathrm{d}y_1 \int \mathrm{d}z_1\, \phi^{\sigma}_{\alpha}(y_1, z_{1\sigma})\mathrm{K}_0\left(|q_x|\sqrt{y_3^2 + (z_3 - z_1)^2}\right)\phi^{\sigma}_{\beta}(y_1, z_{1\sigma}). \tag{12}$$

Assuming zero thickness in the y-direction and considering only the lowest y sub-band to be populated, we write $\phi^{\sigma}_{\alpha}(y_2, z_{2\sigma})\phi^{\sigma}_{\beta}(y_2, z_{2\sigma}) = |\chi(y_2)|^2\xi^{\sigma}_{\alpha}(z_{2\sigma})\xi^{\sigma}_{\beta}(z_{2\sigma}) \approx \delta(y_2)\xi^{\sigma}_{\alpha}(z_{2\sigma})\xi^{\sigma}_{\beta}(z_{2\sigma})$. With this, the polarizability reduces to

$$\begin{aligned}\alpha(y_3 z_3, y_2 z_2; q_x, \omega) &= \delta(y_3 - y_2)\delta(z_3 - z_2)[\eta_+(z_3) - 1] \\ &+ \delta(z_2)\eta_-(z_3)|z_3|(\varepsilon' - \varepsilon)\left(\frac{|q_x|}{2\pi}\right)\left(\frac{\mathrm{K}_1\left(|q_x|\sqrt{(y_2 - y_3)^2 + z_3^2}\right)}{\sqrt{(y_2 - y_3)^2 + z_3^2}}\right) \\ &- 2e^2\delta(y_2) \sum_{\alpha,\beta}\sum_{\sigma} R^{\sigma}_{\alpha\beta}(q_x, \omega)V^{\sigma}_{\alpha\beta}(y_3, z_3)\xi^{\sigma}_{\alpha}(z_{2\sigma})\xi^{\sigma}_{\beta}(z_{2\sigma}).\end{aligned} \tag{13}$$

3. Solution for the inverse dielectric function $K(1,2)$

The inverse dielectric function of the combined system $K(1,2) = \delta V(1)/\delta U(2)$ ($1 = \mathbf{r}_1, t_1$, etc) is determined by the RPA integral equation

$$K(1,2) = \delta^{(4)}(1-2) - \int \mathrm{d}^4 2'\, \alpha(1,2')K(2',2), \tag{14}$$

where the kernel is the polarizability α of equation (13) above. Suppressing q_x and ω, we have

$$\begin{aligned} K(y_1 z_1, y_2 z_2) = {} & \frac{1}{\eta_+(z_1)}\delta(y_1 - y_2)\delta(z_1 - z_2) \\ & - \delta(z_2)\left(\frac{|q_x|\Gamma}{\pi}\right)\left(\frac{\eta_-(z_1)|z_1|}{\eta_+(z_1)}\right)\left(\frac{\mathrm{K}_1\left(|q_x|\sqrt{(y_1-y_2)^2+z_1^2}\right)}{\sqrt{(y_1-y_2)^2+z_1^2}}\right) \\ & + \frac{2e^2}{\varepsilon}\sum_{\alpha,\beta}\sum_{\sigma} R^{\sigma}_{\alpha\beta}K^{\sigma}_{\alpha\beta}(y_1,z_1)\left[\delta(y_2)\xi^{\sigma}_{\alpha}(z_{2\sigma})\xi^{\sigma}_{\beta}(z_{2\sigma}) - \frac{\pi\Gamma}{|q_x|}\delta(z_2)Y^{\sigma}_{\alpha\beta}(y_2)\right], \end{aligned} \tag{15}$$

where we have defined $\Gamma = (\varepsilon' - \varepsilon)/(\varepsilon' + \varepsilon)$ and

$$Y^{\sigma}_{\alpha\beta}(y_2) = \int \mathrm{d}z_3\, |z_3|\xi^{\sigma}_{\alpha}(z_{3\sigma})\left(\frac{\mathrm{K}_1\left(|q_x|\sqrt{y_2^2+z_3^2}\right)}{\sqrt{y_2^2+z_3^2}}\right)\xi^{\sigma}_{\beta}(z_{3\sigma}) \tag{16}$$

(1D quantum wire sub-band wavefunctions are assumed to be wholly confined within the bounding surface, i.e., $z > 0$). The matrix element of the inverse dielectric function denoted by $K^{\sigma}_{\alpha\beta}(y_1, z_1)$ is defined as

$$K^{\sigma}_{\alpha\beta}(y_1,z_1) = \int \mathrm{d}y_3 \int \mathrm{d}z_3\, K(y_1z_1, y_3z_3)V^{\sigma}_{\alpha\beta}(y_3,z_3). \tag{17}$$

Further analysis of this integral equation yields a matrix equation for $K^{\sigma}_{\alpha\beta}(y_1, z_1)$ as

$$\begin{aligned} K^{\rho}_{\mu\nu}(y_1,z_1) = {} & \frac{2e^2}{\varepsilon}\sum_{\alpha,\beta}\sum_{\sigma} R^{\sigma}_{\alpha\beta}\Bigg[\int \mathrm{d}z_2 \int \mathrm{d}z_3\, \xi^{\sigma}_{\alpha}(z_{2\sigma})\xi^{\sigma}_{\beta}(z_{2\sigma})\mathrm{K}_0\left(|q_x||z_2 - z_3|\right)\xi^{\rho}_{\mu}(z_{3\rho}) \\ & \times \xi^{\rho}_{\nu}(z_{3\rho}) - \Gamma\int \mathrm{d}z_2 \int \mathrm{d}z_3\, \xi^{\sigma}_{\alpha}(z_{2\sigma})\xi^{\sigma}_{\beta}(z_{2\sigma})\mathrm{K}_0(|q_x|[|z_2| \\ & + |z_3|])\xi^{\rho}_{\mu}(z_{3\rho})\xi^{\rho}_{\nu}(z_{3\rho})\Bigg]K^{\sigma}_{\alpha\beta}(y_1,z_1) \\ & + \frac{1}{\eta_+(z_1)}\int \mathrm{d}z_2\, \xi^{\rho}_{\mu}(z_{2\rho})\mathrm{K}_0\left(|q_x|\sqrt{y_1^2+(z_1-z_2)^2}\right)\xi^{\rho}_{\nu}(z_{2\rho}) \\ & - \Gamma\frac{\eta_-(z_1)}{\eta_+(z_1)}\int \mathrm{d}z_2\, \xi^{\rho}_{\mu}(z_{2\rho})\mathrm{K}_0\left(|q_x|\sqrt{y_1^2+(|z_1|+|z_2|)^2}\right)\xi^{\rho}_{\nu}(z_{2\rho}). \end{aligned} \tag{18}$$

The inverse dielectric function may be determined explicitly neglecting tunnelling and intersub-band transitions in the quantum wires, which may be expressed as $R^{\sigma}_{\alpha\beta} \to \delta_{\alpha\beta}R^{\sigma}_{\alpha\alpha}$ (due to the suppression of terms with $\alpha \neq \beta$ by relatively large energy denominators). Assuming thin quantum wires ($q_x b \ll 1$, and $|\xi^{\sigma}_{\alpha}(z_{1\sigma})|^2 \to \delta(z_{1\sigma})$) (however, a finite thickness, b, for the quantum wires in the z-direction is necessary to avoid possible divergences in a well defined

physical problem since $\mathrm{K}_0(z) \to -\ln(z/2)$ for small argument z), the matrix equation for the inverse dielectric function becomes

$$K^{\rho}_{\mu\nu}(y_1, z_1) = \delta_{\mu\nu}\left\{\frac{2e^2}{\varepsilon}\sum_{\alpha}\sum_{\sigma} R^{\sigma}_{\alpha\alpha}K^{\sigma}_{\alpha\alpha}(y_1, z_1)\left[\mathrm{K}_0\left(|q_x|a(\sigma-\rho)\right) - \Gamma\mathrm{K}_0\left(|q_x|[z_{0\sigma}+z_{0\rho}]\right)\right]\right.$$
$$\left. + \frac{1}{\eta_+(z_1)}\mathrm{K}_0\left(|q_x|\sqrt{y_1^2+z_{1\rho}^2}\right) - \Gamma\frac{\eta_-(z_1)}{\eta_+(z_1)}\mathrm{K}_0\left(|q_x|\sqrt{y_1^2+(|z_1|+z_{0\rho})^2}\right)\right\}. \quad (19)$$

The appearance of the Kroenecker delta ($\delta_{\mu\nu}$) on the right-hand side above implies that the matrix equation for $K^{\rho}_{\mu\nu}(y_1, z_1)$ is diagonal, such that $K^{\rho}_{\mu\nu}(y_1, z_1) = \delta_{\mu\nu}K^{\rho}_{\mu\mu}(y_1, z_1)$. Thus,

$$K^{\rho}_{\mu\mu}(y_1, z_1) = \frac{2e^2}{\varepsilon}\sum_{\alpha}\sum_{\sigma} R^{\sigma}_{\alpha\alpha}K^{\sigma}_{\alpha\alpha}(y_1, z_1)[\mathrm{K}_0(|q_x|b)\delta_{\sigma\rho} + \mathrm{K}_0(|q_x|a|\sigma-\rho|)(1-\delta_{\sigma\rho})$$
$$- \Gamma(\mathrm{K}_0(2|q_x|[z_0+\sigma a])\delta_{\sigma\rho} + \mathrm{K}_0(|q_x|[2z_0+(\sigma+\rho)a])(1-\delta_{\sigma\rho}))]$$
$$+ N^{\rho}(y_1, z_1), \quad (20)$$

where we have defined N^{ρ}, which is independent of μ, as

$$N^{\rho}(y_1, z_1) = \frac{1}{\eta_+(z_1)}\mathrm{K}_0\left(|q_x|\sqrt{y_1^2+z_{1\rho}^2}\right) - \Gamma\frac{\eta_-(z_1)}{\eta_+(z_1)}\mathrm{K}_0\left(|q_x|\sqrt{y_1^2+(|z_1|+z_{0\rho})^2}\right). \quad (21)$$

In this, we have separated the diagonal ($\sigma = \rho$) log-divergent term $\mathrm{K}_0(|q_x|b)$ from the off-diagonal ($\sigma \neq \rho$) terms $\mathrm{K}_0(|q_x|a|\sigma-\rho|)$. The latter are considerably smaller for $|q_x|b \ll 1$ with $b \ll a$. To solve equation (20), we multiply by $R^{\rho}_{\mu\mu}$ and sum on μ, obtaining

$$\sum_{\sigma}\left(\delta_{\rho\sigma} - \frac{2e^2}{\varepsilon}\sum_{\mu} R^{\rho}_{\mu\mu}f_{\rho\sigma}\right)V^{\sigma}(y_1, z_1) = \tilde{\eta}^{\rho}(y_1, z_1), \quad (22)$$

where we have defined

$$V^{\rho}(y_1, z_1) = \sum_{\mu} R^{\rho}_{\mu\mu}K^{\rho}_{\mu\mu}(y_1, z_1), \quad (23)$$

$$f_{\rho\sigma} = \mathrm{K}_0(|q_x|b)\delta_{\sigma\rho} + \mathrm{K}_0(|q_x|a|\sigma-\rho|)(1-\delta_{\sigma\rho})$$
$$- \Gamma\left[\mathrm{K}_0(2|q_x|[z_0+\sigma a])\delta_{\sigma\rho} + \mathrm{K}_0(|q_x|[2z_0+(\sigma+\rho)a])(1-\delta_{\sigma\rho})\right], \quad (24)$$

and

$$\tilde{\eta}^{\rho}(y_1, z_1) = \sum_{\mu} R^{\rho}_{\mu\mu}N^{\rho}(y_1, z_1). \quad (25)$$

A ρ–σ matrix inversion solution for V^{σ} can be employed in the final determination of $K(y_1z_1, y_2z_2)$ as

$$K(y_1z_1, y_2z_2) = \frac{1}{\eta_+(z_1)}\delta(y_1-y_2)\delta(z_1-z_2)$$
$$- \delta(z_2)\left(\frac{|q_x|\Gamma}{\pi}\right)\left(\frac{\eta_-(z_1)|z_1|}{\eta_+(z_1)}\right)\left(\frac{\mathrm{K}_1\left(|q_x|\sqrt{(y_1-y_2)^2+z_1^2}\right)}{\sqrt{(y_1-y_2)^2+z_1^2}}\right)$$
$$+ \frac{2e^2}{\varepsilon}\sum_{\sigma} V^{\sigma}(y_1, z_1)\left[\delta(y_2)\delta(z_{2\sigma}) - \frac{\pi\Gamma}{|q_x|}\delta(z_2)Y^{\sigma}(y_2)\right], \quad (26)$$

and

$$Y^{\sigma}(y_2) = \int \mathrm{d}z_3\,|z_3|\delta(z_{3\sigma})\left(\frac{\mathrm{K}_1\left(|q_x|\sqrt{y_2^2+z_3^2}\right)}{\sqrt{y_2^2+z_3^2}}\right). \quad (27)$$

4. Interface effects on double-quantum-wire current-driven plasmon instability

To examine the effects of an interface on the criterion for current-driven double-quantum-wire plasmon (DQWP) instability, we consider the DQWP dispersion relation which may be extracted from the homogeneous counterpart of equation (22) as

$$\Delta = \det\left(\delta_{\rho\sigma} - \frac{2e^2}{\varepsilon}\sum_{\mu} R^{\rho}_{\mu\mu} f_{\rho\sigma}\right) = 0. \tag{28}$$

Restricting the double-quantum-wire indices to $\rho, \sigma = 0, 1$ and also restricting population considerations to the lowest sub-band alone (with higher sub-bands taken to be energetically inaccessible), $\sum_{\mu} R^{\rho}_{\mu\mu} \to R^{\rho}$, we have

$$\det\left(\delta_{\rho\sigma} - \frac{2e^2}{\varepsilon} R^{\rho} f_{\rho\sigma}\right) = 0, \tag{29}$$

or, installing R^{ρ} and $f_{\rho\sigma}$ from equations (9) and (24), the DQWP dispersion relation is given by

$$\left[1 - \frac{2e^2}{\varepsilon} V_{00}(q_x)\, R_+(q_x, \omega)\right]\left[1 - \frac{2e^2}{\varepsilon} V_{11}(q_x)\, R_-(q_x, \omega)\right] - \left(\frac{2e^2}{\varepsilon}\right)^2 V_{01}^2(q_x)\, R_+(q_x, \omega)\, R_-(q_x, \omega) = 0 \tag{30}$$

($R^{\sigma} \to R_{\pm}$ for the two wires involved here), where

$$\begin{aligned} V_{00}(q_x) &= \mathrm{K}_0(q_x b) - \Gamma \mathrm{K}_0(2q_x z_0), \\ V_{11}(q_x) &= \mathrm{K}_0(q_x b) - \Gamma \mathrm{K}_0(q_x\,[2z_0 + a]), \\ V_{01}(q_x) &= V_{10}(q_x) = \mathrm{K}_0(q_x a) - \Gamma \mathrm{K}_0(q_x\,[2z_0 + a]). \end{aligned} \tag{31}$$

The role of equal and opposite currents in the two wires is simulated, as in earlier work [19], by introducing associated drifts in the momentum variables of the Fermi equilibrium distribution functions of the two wires ($\rho = 0, 1 \to \pm$), $q_x \to q_x \mp m v_{\mathrm{dr}}/\hbar$. Correspondingly, the density perturbation response functions of equation (9) take the form

$$R_{\pm}(q_x, \omega) = \int \frac{\mathrm{d}k_x}{2\pi} \frac{f_0\left(\epsilon\left(k_x \mp \frac{m v_{\mathrm{dr}}}{\hbar} - q_x\right)\right) - f_0\left(\epsilon\left(k_x \mp \frac{m v_{\mathrm{dr}}}{\hbar}\right)\right)}{\hbar\omega + \epsilon(k_x - q_x) - \epsilon(k_x)}. \tag{32}$$

For low wavenumbers, $q_x < k_{\mathrm{F}}$, this is well approximated by

$$R_{\pm}(q_x, \omega) = \frac{n}{m} \frac{q_x^2}{(\omega \mp q_x v_{\mathrm{dr}})^2 - q_x^2 v_{\mathrm{F}}^2}, \tag{33}$$

which would also emerge from a semiclassical treatment in terms of a linearized classical collisionless Vlasov–Boltzmann equation with averaging against a sharply cut off Fermi–Dirac distribution function. Substituting equation (33) for $R_{\pm}$ into the dispersion relation, equation (30), we obtain

$$\left(1 - \frac{q_x^2 u_0^2}{(\omega - q_x v_{\mathrm{dr}})^2 - q_x^2 v_{\mathrm{F}}^2} V_{00}\right)\left(1 - \frac{q_x^2 u_0^2}{(\omega + q_x v_{\mathrm{dr}})^2 - q_x^2 v_{\mathrm{F}}^2} V_{11}\right) - \frac{q_x^2 u_0^2}{(\omega - q_x v_{\mathrm{dr}})^2 - q_x^2 v_{\mathrm{F}}^2} \frac{q_x^2 u_0^2}{(\omega + q_x v_{\mathrm{dr}})^2 - q_x^2 v_{\mathrm{F}}^2} V_{10}^2 = 0, \tag{34}$$

or

$$\left[(\omega - q_x v_{\mathrm{dr}})^2 - q_x^2 v_{\mathrm{F}}^2 - q_x^2 u_0^2 V_{00}\right]\left[(\omega + q_x v_{\mathrm{dr}})^2 - q_x^2 v_{\mathrm{F}}^2 - q_x^2 u_0^2 V_{11}\right] - \left(q_x^2 u_0^2\right)^2 V_{10}^2 = 0, \tag{35}$$

where $u_0^2 = 2ne^2/m\varepsilon$. The role of the surface is embedded in the V s of equation (31), which, in turn, determine the mode spectrum dependence on z_0 through equation (35), which may also be written as

$$\omega^4 - \left[2q_x^2\left(v_{\rm dr}^2 + v_{\rm F}^2\right) + q_x^2u_0^2\left(V_{00} + V_{11}\right)\right]\omega^2 + 2\left(q_xv_{\rm dr}\right)\left(q_x^2u_0^2\right)\left(V_{11} - V_{00}\right)\omega + q_x^4\left(v_{\rm dr}^2 - v_{\rm F}^2 - u_0^2V_{00}\right)\left(v_{\rm dr}^2 - v_{\rm F}^2 - u_0^2V_{11}\right) - \left(q_xu_0\right)^4V_{10}^2 = 0. \tag{36}$$

This dispersion relation is quartic in ω and, while it can be solved exactly, it simplifies considerably when $a \ll z$ since the term involving $(V_{11} - V_{00})$ may then be neglected and the quartic dispersion relation simply becomes quadratic in ω^2. Considering this case, we have

$$\omega_\pm^2 = q_x^2\left(v_{\rm dr}^2 + v_{\rm F}^2 + u_0^2V_{00}\right) \pm q_x^2\sqrt{4v_{\rm dr}^2\left(v_{\rm F}^2 + u_0^2V_{00}\right) + u_0^4V_{10}^2}. \tag{37}$$

The corresponding plasmon dispersion relation in the absence of drift has acoustic (−) and optical (+) plasmon branches with coupling to bulk and surface plasmons and/or phonons of the host through Γ which incorporates such structure in $\epsilon(\omega)$,

$$\omega_\pm^2 = q_x^2\left[v_{\rm F}^2 + u_0^2\left(V_{00} \pm V_{10}\right)\right]. \tag{38}$$

Alternatively, these modes are given by ($\Gamma \to \Gamma(\omega) = (\varepsilon'(\omega) - \varepsilon(\omega))/(\varepsilon'(\omega) + \varepsilon(\omega))$),

$$\omega_\pm^2 = q_x^2\left\{v_{\rm F}^2 + u_0^2\left[\left(K_0\left(q_xb\right) - \Gamma K_0\left(2q_xz_0\right)\right) \pm \left(K_0\left(q_xa\right) - \Gamma K_0\left(q_x\left[2z_0 + a\right]\right)\right)\right]\right\}. \tag{39}$$

Instability arises then when $\omega_\pm^2 < 0$, which occurs when

$$\sqrt{v_{\rm F}^2 + u_0^2\left(V_{00} - V_{10}\right)} < v_{\rm dr} < \sqrt{v_{\rm F}^2 + u_0^2\left(V_{00} + V_{10}\right)}. \tag{40}$$

In is clear that plasma mode instability occurs when $v_{\rm dr}$ falls between the acoustic and optical mode phase velocities;

$$v_{\rm p-}\left(q_x\right) < v_{\rm dr} < v_{\rm p+}\left(q_x\right). \tag{41}$$

To gain an appreciation of the role of the surface, we start by eliminating the bulk and surface modes by choosing both ε and ε' to be constants, $\varepsilon' = 1$ and $\varepsilon = 13$, and exhibit the resulting instability range in figure 2 (for a given q_x, the instability range of $v_{\rm dr}/v_{\rm F}$ extends from the lower (acoustic) plasmon phase velocity to the upper (optical) one). The parameters involved are $z_0 = 200$ nm, $a = 30$ nm and $b = 15$ nm. For comparison purposes, we include an inset in figure 2 showing the corresponding results when the adjoining region is AlGaAs rather than vacuum with $z_0 = 60$ nm, $a = 3$ nm and $b = 1.5$ nm. In both cases of $\varepsilon' = 1$ and 10, the range of instability increases as q_x decreases. It is of particular interest to note that the instability limits of $v_{\rm dr}/v_{\rm F}$ as a function of z_0 in figure 3 show that the instability range increases mainly because the optical plasmon phase velocity increases more than that of the acoustic mode as z_0 decreases (in figure 3, $\varepsilon' = 1$, $\varepsilon = 13$, $a = 30$ nm, $b = 15$ nm and $q_x = 1 \times 10^5$ cm). Naturally, as z_0 increases, the effect of the image (boundary) on the instability range is diminished.

5. Undrifted N-quantum-wire plasmon spectroscopy: general considerations with bulk and surface mode interactions

Considering next the general problem of N quantum wires (without drift) in a plasma-like medium with the first one at a distance z_0 from the interface, the frequency poles of the inverse dielectric function of equation (26) (given by the dispersion relation of equation (28)) describe the coupled plasmons of the joint system. The decoupled bulk and surface plasmons are evident in the frequency poles of equation (26) as the vanishings of $\varepsilon = \varepsilon_0 - \omega_{\rm p}^2/\omega^2$ and

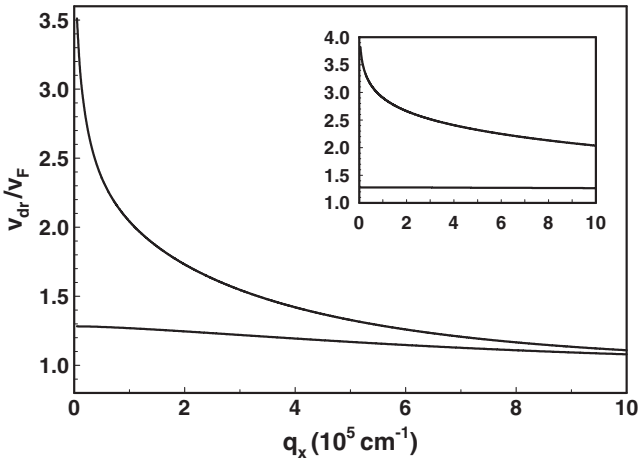

Figure 2. Drift velocity instability regime as a function of q_x for a vacuum–GaAs interface with $\varepsilon' = 1$, $\varepsilon = 13$, $z_0 = 200$ nm, $a = 30$ nm and $b = 15$ nm. Inset: drift velocity instability regime as a function of q_x for an AlGaAs–GaAs interface with $\varepsilon' = 10$, $\varepsilon = 13$, $z_0 = 60$ nm, $a = 3$ nm and $b = 1.5$ nm.

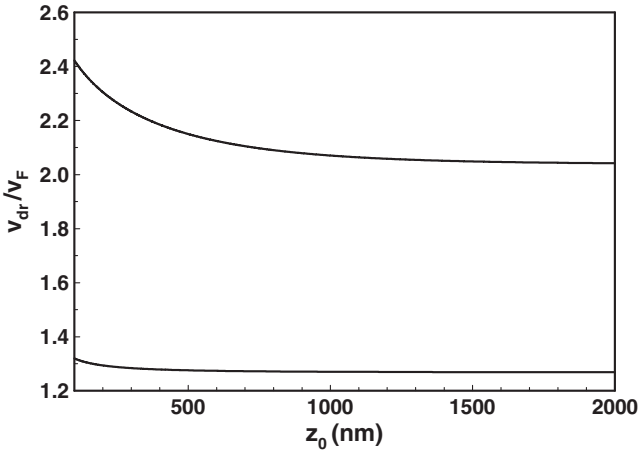

Figure 3. Drift velocity instability regime as a function of z_0 for a vacuum–GaAs interface with $\varepsilon' = 1$, $\varepsilon = 13$, $q_x = 1 \times 10^5$ cm, $a = 30$ nm and $b = 15$ nm.

$1/\Gamma = (\varepsilon' + \varepsilon)/(\varepsilon' - \varepsilon)$, which introduce the bulk and surface modes as $\omega^2 = \omega_p^2/\varepsilon_0$ and $\omega_s^2 = \omega_p^2/(\varepsilon' + \varepsilon)$, respectively. These modes are always in the spectrum.

In addition, equation (26) for $K(y_1 z_1, y_2 z_2)$ has coupled plasmon poles for the joint system determined by

$$\Delta = \det\left(\delta_{\rho\sigma} - \frac{2e^2}{\varepsilon}\sum_{\mu} R^{\rho}_{\mu\mu} f_{\rho\sigma}\right) = 0. \tag{42}$$

Taking all the wires to be identical, $R^{\rho}_{\mu\mu} = R_{\mu\mu}$ is independent of the wire index ρ. Furthermore, we consider the case in which only the lowest sub-band is populated, so that $R_{\mu\mu} = \delta_{\mu 0} R$. For the local cold plasma limit, we obtain the common density perturbation response function for the quantum wires as $R = n_{1D} q_x^2/(m\omega^2)$, where n_{1D} is the 1D equilibrium

density (number of electrons per unit length) of the quantum wires. Also, in the local limit $\varepsilon = \varepsilon_0 - \omega_{\rm p}^2/\omega^2$.

In the case of a single quantum wire, i.e. $N = 1$, and in the absence of an interface, $\Gamma = 0$, and $\varepsilon = \varepsilon_0$ is a constant, we have

$$\omega^2 = \omega_{\rm 1D}^2 = \left(\frac{2e^2 n_{\rm 1D}}{\varepsilon_0 m}\right) q_x^2 {\rm K}_0(|q_x|b). \tag{43}$$

This is the known dispersion relation for a one-dimensional (1D) quantum wire [4–6] embedded in a constant dielectric host medium. For the case when $\varepsilon = \varepsilon_0 - \omega_{\rm p}^2/\omega^2$, it becomes

$$\omega^2 = \left(\frac{\omega_{\rm p}^2}{\varepsilon_0}\right) + \left(\frac{2e^2 n_{\rm 1D}}{\varepsilon_0 m}\right) q_x^2 {\rm K}_0(|q_x|b), \tag{44}$$

which indicates the hybridization of the 1D quantum wire plasmon with the local bulk host plasmon. On the other hand, if an interface is considered, the dispersion relation takes the form

$$\begin{aligned}\omega_\pm^2 = \left(\frac{1}{2}\right)\Bigg\{&\left(\frac{\omega_{\rm p}^2}{\varepsilon_0}\right) + \omega_{\rm s}^2 + \left(\frac{2e^2 n_{\rm 1D}}{\varepsilon_0 m}\right) q_x^2 ({\rm K}_0(|q_x|b) - \gamma {\rm K}_0(2|q_x|z_0)) \\ &\pm \Bigg(\left[\left(\frac{\omega_{\rm p}^2}{\varepsilon_0}\right) + \omega_{\rm s}^2 + \left(\frac{2e^2 n_{\rm 1D}}{\varepsilon_0 m}\right) q_x^2 ({\rm K}_0(|q_x|b) - \gamma {\rm K}_0(2|q_x|z_0))\right]^2 \\ &- 4\omega_{\rm s}^2\left[\left(\frac{\omega_{\rm p}^2}{\varepsilon_0}\right) + \left(\frac{2e^2 n_{\rm 1D}}{\varepsilon_0 m}\right) q_x^2 ({\rm K}_0(|q_x|b) + {\rm K}_0(2|q_x|z_0))\right]\Bigg)^{1/2}\Bigg\},\end{aligned} \tag{45}$$

where $\gamma = (\varepsilon' - \varepsilon_0)/(\varepsilon' + \varepsilon_0)$ is independent of frequency. We note that this dispersion relation for the quantum wire in the presence of an interface describes two modes which depend on z_0, the distance of the wire centre from the interface. When it is far from the interface ($z_0 \to \infty$), the 'upper' mode reproduces the hybridization of the bulk plasmon with the 1D quantum wire plasmon, equation (44), and the 'lower' mode is a decoupled surface plasmon, $\omega_{\rm s}$. The other limit, in which the quantum wire approaches the interface but still remains within the bounding surface ($z_0 \to b/2$), yields

$$\omega_\pm^2 = \left(\frac{1}{2}\right)\left\{\left(\frac{\omega_{\rm p}^2}{\varepsilon_0}\right) + \omega_{\rm s}^2 + \overline{\omega}_{\rm 1D}^2 \pm \left|\left(\frac{\varepsilon'}{\varepsilon_0}\right)\omega_{\rm s}^2 - \overline{\omega}_{\rm 1D}^2\right|\right\}, \tag{46}$$

where

$$\overline{\omega}_{\rm 1D}^2 = \left(\frac{2e^2 n_{\rm 1D}}{\overline{\varepsilon} m}\right) q_x^2 {\rm K}_0(|q_x|b) \tag{47}$$

is similar to the 1D plasma frequency of the quantum wire given in equation (43), but with an average of the dielectric constants of the bounding surface and the host medium, $\overline{\varepsilon} = (\varepsilon' + \varepsilon_0)/2$, replacing ε_0 at the interface. For a constant dielectric background ($\varepsilon = \varepsilon_0$), equation (45) reduces to

$$\omega_+^2 = \left(\frac{2e^2 n_{\rm 1D}}{\varepsilon_0 m}\right) q_x^2 \left({\rm K}_0(|q_x|b) - \gamma {\rm K}_0(2|q_x|z_0)\right), \qquad \omega_-^2 = 0. \tag{48}$$

For large values of z_0 ($z_0 \to \infty$) it becomes $\omega_{\rm 1D}^2$, equation (43), and for $z_0 \to b/2$ it becomes $\overline{\omega}_{\rm 1D}^2$, equation (47).

For an arbitrary number of wires, N, it is convenient to rewrite the dispersion relation, equation (42), in the general form $\Delta = \det M^{\rho\sigma} = 0$, where

$$\begin{aligned}M^{\rho\sigma} = \delta_{\rho\sigma} - \frac{2e^2}{\varepsilon} R^\sigma \{&{\rm K}_0(|q_x|b)\delta_{\rho\sigma} + {\rm K}_0(|q_x|a|\sigma - \rho|)(1 - \delta_{\rho\sigma}) \\ &- \Gamma[{\rm K}_0(2|q_x|[z_0 + \sigma a])\delta_{\rho\sigma} + {\rm K}_0(|q_x|[2z_0 + (\sigma + \rho)a])(1 - \delta_{\rho\sigma})]\}.\end{aligned} \tag{49}$$

There is considerable simplification for $|q_x|b < 1$ in the case when $z_0 \gg Na \gg Nb$, since we can then neglect $K_0(|q_x|a|\sigma - \rho|)(1 - \delta_{\rho\sigma})$ compared to $K_0(|q_x|b)$ and the terms involving the image factor, Γ, combine to $K_0(2|q_x|z_0)$, with the result

$$M^{\rho\sigma} = \left[1 - \frac{2e^2}{\varepsilon} R K_0(|q_x|b)\right]\delta_{\rho\sigma} - \frac{2e^2}{\varepsilon} R\Gamma K_0(2|q_x|z_0). \tag{50}$$

The last term on the right is relatively small and negligible under the conditions already stated, and it may be discarded *except* in the frequency region where $\Gamma \gg 1$, where it describes coupling of the quantum-wire modes to the surface plasmon. The structure of M and its determinant are discussed in detail in the appendix. The resulting dispersion relation for $z_0 \gg Na$ involves two distinct sets of modes. One set arises from the quadratic equation

$$1 - \frac{2e^2}{\varepsilon} R K_0(|q_x|b) - \frac{2e^2}{\varepsilon} R\Gamma K_0(2|q_x|z_0) = 0, \tag{51}$$

which has two roots given by

$$\begin{aligned}\omega_{\pm}^2 = \left(\frac{1}{2}\right)\Bigg\{&\left(\frac{\omega_p^2}{\varepsilon_0}\right) + \omega_s^2 + \left(\frac{2e^2 n_{1D}}{\varepsilon_0 m}\right) q_x^2 (K_0(|q_x|b) - \gamma N K_0(2|q_x|z_0)) \\ &\pm \Bigg(\left[\left(\frac{\omega_p^2}{\varepsilon_0}\right) + \omega_s^2 + \left(\frac{2e^2 n_{1D}}{\varepsilon_0 m}\right) q_x^2 (K_0(|q_x|b) - \gamma N K_0(2|q_x|z_0))\right]^2 \\ &- 4\omega_s^2\left[\left(\frac{\omega_p^2}{\varepsilon_0}\right) + \left(\frac{2e^2 n_{1D}}{\varepsilon_0 m}\right) q_x^2 (K_0(|q_x|b) + N K_0(2|q_x|z_0))\right]\Bigg)^{1/2}\Bigg\},\end{aligned} \tag{52}$$

where $\gamma = (\varepsilon' - \varepsilon_0)/(\varepsilon' + \varepsilon_0)$ is independent of frequency. It should be noted that in the present case, with $z_0 \gg Na$, the N wires behave as if they are clustered into a single wire (with a corresponding decoupling of the surface plasmon) and hybridization of the bulk plasmon with the single-quantum-wire plasmon has a strength factor N.

The second set of modes, given by

$$\left(1 - \frac{2e^2}{\varepsilon} R K_0(|q_x|b)\right)^{N-1} = 0, \tag{53}$$

yields a $2(N-1)$-degenerate-mode dispersion relation,

$$\omega^2 = \left(\frac{\omega_p^2}{\varepsilon_0}\right) + \left(\frac{2e^2 n_{1D}}{\varepsilon_0 m}\right) q_x^2 K_0(|q_x|b), \tag{54}$$

which is characteristic of a single-quantum-wire plasmon hybridized with a bulk plasmon, for the case in which $z_0 \gg Na$ so that the interface image is not felt. It is worthwhile to note that the $(N-1)$ degeneracy of this mode, which is obviated in the appendix, will clearly be doubled with the doubling of ω^2 roots by the inclusion of a small measure of nonlocality so that the local limit has $2(N-1)$ degenerate modes. Considering both sets of modes, we therefore correctly have a total of $2 + 2(N-1) = 2N$. We examined the limit $z_0 \gg Na$ in detail in [14].

6. Conclusions: numerical analysis of the dispersion relation

We have explicitly constructed the inverse dielectric function of an N-quantum-wire system embedded in a dynamic host medium in the vicinity of a bounding surface, equation (26), and have derived the dispersion relation for the coupled modes of this system, equation (28). This formulation has been applied to a double-quantum-wire system with equal and opposite drift velocities in the two wires in the vicinity of an interface. In this application, we neglected both

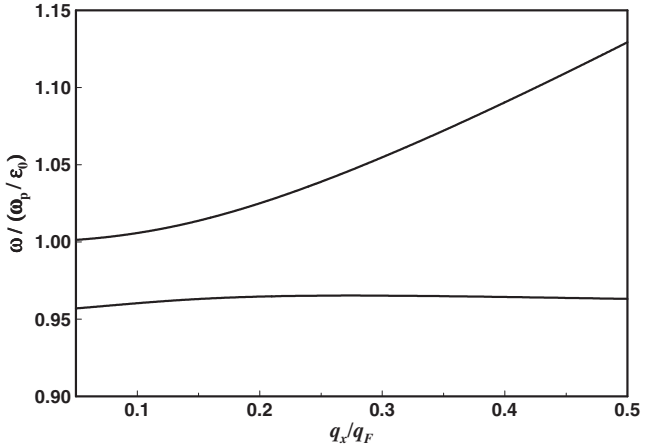

Figure 4. Plot of $\omega/(\omega_{\rm p}/\sqrt{\varepsilon_0})$ as a function of $q_x/q_{\rm F}$ for $z_0 = 50$ Å, $N = 1$ wire and a vacuum–GaAs interface.

plasma-like and phonon-like excitations of the host medium. The range of drift velocities which drive the acoustic and optical plasmons of the double-wire system unstable was obtained as a function of wavenumber along the wire (q_x) and distance (z_0) from the interface. In particular, we confirmed that such instability occurs when the drift velocity magnitude falls between the acoustic and optical plasmon phase velocities, and found that this range increases as z_0 decreases since the optical mode phase velocity increases more rapidly than that of the acoustic mode phase velocity as $z_0 \to 0$.

Considering the general case of N wires with *no* restriction on z_0 and *no* drift currents, the dispersion relation is

$$\Delta = \det M^{\rho\sigma} = 0, \tag{55}$$

with $M^{\rho\sigma}$ given by equation (49). Again, there is a total of $2N$ longitudinal electrostatic modes, two for each quantum wire coupled to the semi-infinite dynamic plasma-like medium (as well as being coupled to each other). On the basis of equation (55), we have numerically calculated the coupled plasmon spectrum for the wires coupled to bulk and surface plasmons, determining the collective mode frequencies $\omega/(\omega_{\rm p}/\varepsilon_0^{1/2})$ as functions of $q_x/q_{\rm F}$ for $N = 2, 6$ for $z_0 = 50$ Å. We also exhibit the geometric dependence of $\omega/(\omega_{\rm p}/\varepsilon_0^{1/2})$ as a function of z_0 for $N = 2, 6$ and $q_x/q_{\rm F} = 0.1$. The results shown are for vacuum–GaAs parameter values, $n_{\rm 3D} = 1 \times 10^{24}$ m^{-3}, $n_{\rm 1D} = 1 \times 10^{8}$ m^{-1}, $m = 0.063\, m_{\rm e}$, $\varepsilon' = 1.00$, $\varepsilon_0 = 10.33$, $b = 10$ Å, $a = 20$ Å and $q_{\rm F} = \pi n_{\rm 1D}/2$ is the 1D Fermi wavenumber.

In the case of $N = 1$ wire, figure 4 exhibits the dispersion of the two modes of equation (45) for $z_0 = 50$ Å, representing the coupling of the 1D single-quantum-wire plasmon with the plasmon of the semi-infinite host bulk plasma. For $N = 2$, there are four modes arising from equations (49) and (55) whose dispersion is plotted in figure 5 for $z_0 = 50$ Å. Figure 6 exhibits their dependence on z_0 in this range for $q_x/q_{\rm F} = 0.1$, in which case $z_0 \gg Na = 40$ Å is well satisfied for $z_0 > 500$ Å. Under these conditions the two lowest modes converge to the twofold degenerate frequency of equation (54), while the two upper modes flatten out in accordance with the decline of $K_0(2|q_x|z_0)$ relative to $K_0(|q_x|b)$ (representing the lesser importance of the image term as z_0 becomes large). We have also examined the coupled quantum-wire plasmon spectrum of equations (49) and (55) for $N > 2$ up to $N = 6$, for which case the dispersion is plotted in figure 7 for $z_0 = 50$ Å. There are 12 modes, with five embedded in the lowest

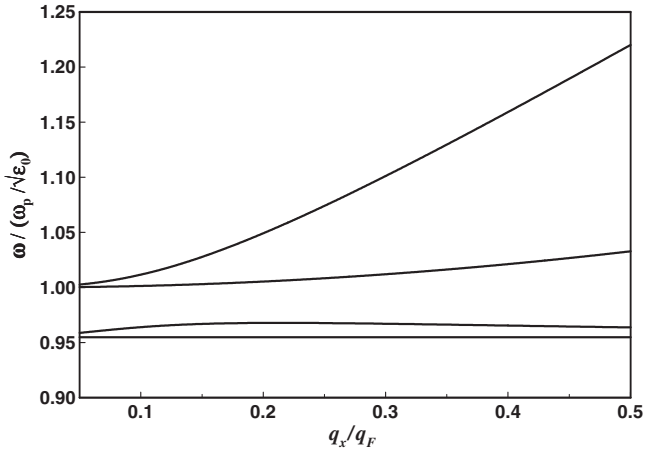

Figure 5. Plot of $\omega/(\omega_{\rm p}/\sqrt{\varepsilon_0})$ as a function of $q_x/q_{\rm F}$ for $z_0 = 50$ Å, $N = 2$ wires and a vacuum–GaAs interface.

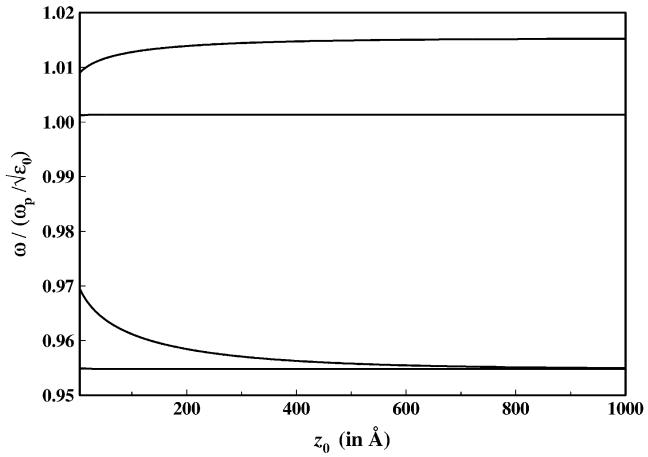

Figure 6. Plot of $\omega/(\omega_{\rm p}/\sqrt{\varepsilon_0})$ as a function of z_0 for $q_x/q_{\rm F} = 0.1$, $N = 2$ wires and a vacuum–GaAs interface.

curve—indistinguishable due to lack of resolution. Figure 8 shows the dependence of these 12 modes on z_0 up to $z_0 = 900$ Å for $q_x/q_{\rm F} = 0.1$, with the 12 clustering into three groups of modes for $z_0 > 600$ Å. Such clustering may be expected on the basis of equations (52)–(54), with two distinct modes from equation (52) and two clusters of five modes each from the degenerate roots of equations (53) and (54) (with one accidental degeneracy in three distinct clusters instead of four).

Our determination of $K(1, 2)$ for an N-quantum-wire system embedded in a dynamic host medium in the vicinity of an interface can also be used to examine the coupled mode spectrum of the wire system plasmons hybridized with bulk and surface phonons as well as plasmons of the dynamic host.

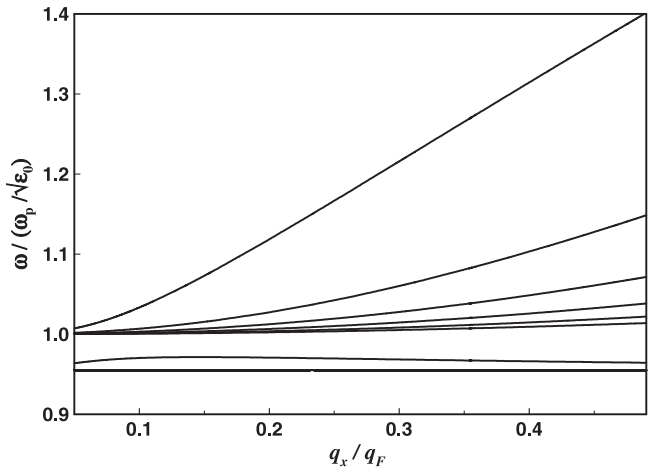

Figure 7. Plot of $\omega/(\omega_{\rm p}/\sqrt{\varepsilon_0})$ as a function of $q_x/q_{\rm F}$ for $z_0 = 50$ Å, $N = 6$ wires and a vacuum–GaAs interface.

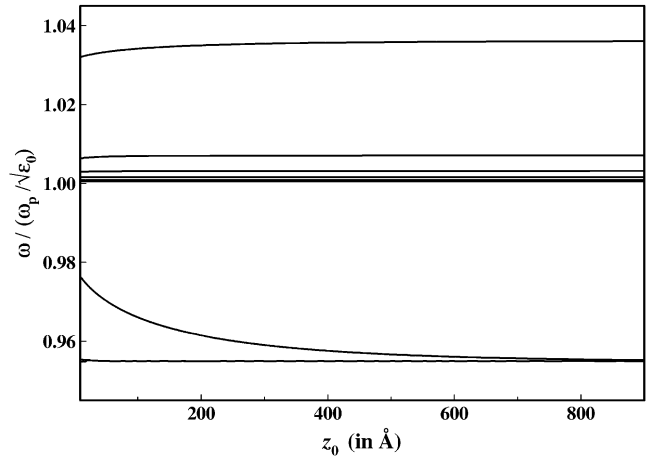

Figure 8. Plot of $\omega/(\omega_{\rm p}/\sqrt{\varepsilon_0})$ as a function of z_0 for $q_x/q_{\rm F} = 0.1$, $N = 6$ wires and a vacuum–GaAs interface.

Acknowledgments

The authors thank Professor G R Aizin for helpful comments, and NJMH gratefully acknowledges support from the US DOD, DAAD 19-01-1-0592.

Appendix

In this appendix, using elementary row (column) operations, we evaluate the determinant of matrix M, equation (50). Introducing A as the diagonal part of M, i.e.,

$$A = 1 - \frac{2e^2}{\varepsilon} R{\rm K}_0\left(|q_x|b\right), \tag{A.1}$$

and B as the constant term of M, i.e.,

$$B = -\frac{2e^2}{\varepsilon} R\Gamma \mathrm{K}_0\left(2|q_x|z_0\right), \tag{A.2}$$

we write M explicitly as

$$M = \begin{pmatrix} A+B & B & B & B & \cdots & B & B \\ B & A+B & B & B & \cdots & B & B \\ B & B & A+B & B & \cdots & B & B \\ B & B & B & A+B & \cdots & B & B \\ \vdots & \vdots & \vdots & \vdots & \ddots & \vdots & \vdots \\ B & B & B & B & \cdots & A+B & B \\ B & B & B & B & \cdots & B & A+B \end{pmatrix}. \tag{A.3}$$

Using the property that the value of the determinant of a matrix is unchanged when we add to/subtract from each element of a row (column) a constant multiple of the corresponding element of another row (column), we subtract the first row of M from all other rows to obtain

$$\det M = \det \begin{pmatrix} A+B & B & B & B & \cdots & B & B \\ -A & A & 0 & 0 & \cdots & 0 & 0 \\ -A & 0 & A & 0 & \cdots & 0 & 0 \\ -A & 0 & 0 & A & \cdots & 0 & 0 \\ \vdots & \vdots & \vdots & \vdots & \ddots & \vdots & \vdots \\ -A & 0 & 0 & 0 & \cdots & A & 0 \\ -A & 0 & 0 & 0 & \cdots & 0 & A \end{pmatrix}. \tag{A.4}$$

Next, we add the first column to the sum of all other columns, obtaining an upper triangular determinant

$$\det M = \det \begin{pmatrix} A+NB & B & B & B & \cdots & B & B \\ 0 & A & 0 & 0 & \cdots & 0 & 0 \\ 0 & 0 & A & 0 & \cdots & 0 & 0 \\ 0 & 0 & 0 & A & \cdots & 0 & 0 \\ \vdots & \vdots & \vdots & \vdots & \ddots & \vdots & \vdots \\ 0 & 0 & 0 & 0 & \cdots & A & 0 \\ 0 & 0 & 0 & 0 & \cdots & 0 & A \end{pmatrix}, \tag{A.5}$$

whose value equals the product of its diagonal elements,

$$\det M = A^{N-1}\left(A+NB\right). \tag{A.6}$$

Finally substituting for A and B, we obtain

$$\det M = \left(1 - \frac{2e^2}{\varepsilon} R\mathrm{K}_0\left(|q_x|b\right)\right)^{N-1} \left[1 - \frac{2e^2}{\varepsilon} R\mathrm{K}_0\left(|q_x|b\right) - \frac{2e^2}{\varepsilon} NR\Gamma \mathrm{K}_0\left(2|q_x|z_0\right)\right]. \tag{A.7}$$

References

[1] Ando T, Fowler A B and Stern F 1982 *Rev. Mod. Phys.* **54** 437

[2] Heitmann D 2004 *Collective and Single Particle Excitations in 3-,2-,1- and 0-Dimensional Electronic Systems* at press

[3] Sanomirskii V B, Volkov V A, Aizin G R and Mikhailov S A 1989 *Electrochim. Acta* **34** 3

[4] Mohan M M and Griffin A 1985 *Phys. Rev.* B **32** 2030

[5] Li Q P and Das Sarma S 1989 *Phys. Rev.* B **40** 5860

[6] Li Q P and Das Sarma S 1991 *Phys. Rev.* B **43** 11768

[7] Wang J and Leburton J P 1990 *Phys. Rev.* B **41** 7846

[8] Gold A and Ghazali A 1990 *Phys. Rev.* B **41** 7626
[9] Mendoza B S and Schaich W L 1991 *Phys. Rev.* B **43** 6590
[10] Demel T, Heitmann D, Grambow P and Ploog K 1991 *Phys. Rev. Lett.* **66** 2657
[11] Sirenko Y M, Vasilopoulos P and Boiko I I 1991 *Phys. Rev.* B **44** 10724
[12] Agosti D, Pederiva F, Lipparini E and Takayanagi K 1998 *Phys. Rev.* B **57** 14869
[13] Wendler L and Grigoryan V G 1994 *Phys. Status Solidi* b **181** 133
[14] Horing N J M, Jena T, Cui H L and Mancini J D 1996 *Phys. Rev.* B **54** 2785
[15] Ayaz Y, Horing N J M, Fessatidis V, Mancini J D and Chen T H 2000 *Microelectron. Eng.* **51/52** 219
[16] Peralta X G, Allen S J, Wanke M C, Harff N B, Simmons J A, Lily M P, Reno J L, Burke P J and Eisenstein J P 2002 *Appl. Phys. Lett.* **81** 1627
[17] Peralta X G, Allen S J, Wanke M C, Simmons J A, Lily M P, Reno J L, Burke P J and Eisenstein J P 2004 *Proc. 26th Int. Conf. on the Physics of Semiconductors* at press
[18] Popov V V, Polischuk O V, Teperik T V, Peralta X G, Allen S J, Horing N J M and Wanke M C 2004 *J. Appl. Phys.* at press
[19] Aizin G R, Horing N J M and Mourokh L G 2002 *Phys. Rev.* B **65** 241311
[20] Horing N J M, Gumbs G and Park T 2001 *Physica* B **299** 165